Numerical investigation of height impact of local exhaust combined with an office work station on energy saving and indoor environment

Ahmed Qasim Ahmed*, Shian Gao

Department of Engineering, University of Leicester, Leicester LE1 7RH, United Kingdom

*Corresponding author: phone: +44(0)116 252 2874; fax: +44(0)116 252 2525; e-mail: aqaa2@ le.ac.uk.

Abstract:

A healthy and comfortable working environment is very important for improving its occupants' productivity. In this study, the evaluation of the height impact for the proposed local exhaust ventilation system on the indoor thermal comfort, inhaled air quality and energy savings was explored numerically. In the proposed system, the exhaust opening was combined with the office workstation in a single unit. The intention was to help extract the warmed and contaminated air locally before it disperses across the room. The performance of the new system at three different heights of the combined system (1.4 m, 1.6 m and 2.0 m) above floor level was investigated numerically with a validated CFD model in a room with and without inclusion of the novel local exhaust ventilation system. The performance of using this system was evaluated using the main evaluation indices for any ventilation system such as energy saving, occupant thermal comfort, draught risk and the quality of the indoor air. The results showed that by selecting a suitable height for the combined system, a significant improvement on energy savings (up to 22.56%) and inhaled air quality can be realised with an acceptable level of the indoor thermal comfort. It was found that in comparison to cases 2 (1.4 m) and 4 (2.0 m), case 3 (1.6 m) was considered to be the best height at which optimal performance could be achieved from the LEVO system.

Keywords: Energy saving, Thermal comfort, Local exhaust ventilation, Displacement ventilation

Nomenclature

Abbreviations

DV	Displacement Ventilation
IAQ	Indoor Air Quality
LEV	Local Exhaust Ventilation
LEVO	Local Exhaust Ventilation for Office
STRAD	Stratified Air Distribution System
PD	Percentage Dissatisfied people
PV	Personal velocity
UFAD	underfloor air distribution system

Latin letters

C	mean particle concentration (kg/m^3)
$C_{1\varepsilon}, C_{2\varepsilon}$	model constants in the term ε of the turbulence model
C_n	normalised concentration.
C_p	contaminant concentration in a specific region (kg/m^3)
C_e	the concentration at exhaust (kg/m^3)
C_μ	model constant of the turbulence model
c_p	specific heat of air (J/(kg k)
d_p	particle diameter (m)
dt	particle residence time
F_D	inverse of relaxation time (1/s)
$\vec{F}_a$	force acting on particle (m/s^2)
$\vec{F}_b$	Brownian force (m/s^2)
$\vec{F}_s$	Saffman's lift forces (m/s^2)
$\vec{g}$	gravitational acceleration (m/s^2)
i	trajectory index
j	cell index
k	turbulent kinetic energy per unit mass (J/kg)
$\dot{m}$	mass flow rate associated with each trajectory (kg/s)
$\dot{m}_e$	exhaust mass flow rate (kg/s)
n	trajectory number
P_k	additional term in the turbulence model
$Q_{coil-STRAD}$	cooling coil load for the STRAD system (W)
Q_{space}	cooling coil load of space (W)
Q_{vent}	ventilation load (W)
$Q_{coil-MV}$	cooling coil load for the mixing ventilation system (W)
S	mean strain rate tensor magnitude
S_{ij}	strain rate tensor
T	air temperature (℃)
T_u	turbulent intensity
T_e	the exhaust temperature (℃)
T_{set}	room set temperature (℃)
t	time (s)
$\vec{u}_p$	particle velocity vector (m/s)
u	fluid velocity (m/s)
u_i'	fluctuating velocity (m/s)
V_j	volume associated with i trajectory and cell j

Greek letters

β	coefficient of thermal expansion (1/K)
ε	turbulent dissipation rate (m^2/s^3)
λ	represents the molecular mean free path
μ	dynamic viscosity (kg/(m s)
ξ_i	normally distributed random number
ρ	fluid density (kg/m^3)
ρ_p	particle density (kg/m^3)
σ_k	model constant for k equation of the turbulence model
σ_ε	model constant for ε equation of the turbulence model

1 Introduction

Thermal comfort and human activity in offices spaces are highly influenced by the indoor thermal environment and the quality of inhaled air [1-3]. In order to provide a healthy and comfortable environment with a low energy consumption, various ventilation strategies such as the local exhaust ventilation (LEV) system or personal ventilation system (PV) have been developed to be used as alternatives to traditional ventilation systems [4-7]. Indoor thermal comfort, indoor air quality and energy savings are affected by many parameters in any ventilation system [8]. One of the principle affecting factors is the locations of the inlet and outlet openings. Furthermore, optimal selection of the return and exhaust opening positions have a considerable impact on the indoor thermal environment and energy saving [9-11]. Junjing et al. [12] examined two different ventilation systems with openings at 12 different positions. In their study, a novel ventilation system, the Personalized Ventilation–Personalized Exhaust (PV-PE) system, was combined with the occupant's chair and located above their shoulder. They found that using this new system can enhance the indoor thermal comfort and quality of the inhaled air. Halvonová and Melikov [13] investigated the performance of the combination of the ductless personalised ventilation (PCV) system and displacement ventilation (DV) system in a room. The results show that this system can provide good inhaled-air quality compared with a room that is not using this system. Kanaan et al. [14] studied the impacts in this regard using a combined DV and PV system in a room on the quality of the inhaled air. The quality of the indoor air was evaluated using CO_2 concentration. They found that the quality of the inhaled air was improved by up to 20% when using the supply air temperature for the DV system at 18 ^oC and for the PV system with a supply air temperature between 18 and 22 ^oC, and a flow rate between 4 L/s to 10 L/s. Yang et al. [15] examined the performance of three different devices of the Personalized Exhaust (PE) system. Their results show that an improvement of the inhaled air quality was achieved when the PE system was located at a level near the shoulder

of the occupant. Neilsen et al. [16] considered the risk of cross-contamination in a hospital ward using a downward ventilation system. They found that the location of the return openings played an important role in the transmission of exhaled contaminants within the ward. Cheong and Phua [17] investigated performance towards contaminant removal using different ventilation systems for a hospital ward. Their results show that the performance in terms of removal of contaminants was enhanced significantly when the supply and exhaust openings were located in the wall near the patient's bed.

Fong et al. [18] performed an experimental study using three different ventilation systems with six different exhaust configurations to investigate the impact of these systems on the indoor thermal environment and energy consumption. Their results show that significant improvements in thermal comfort and energy consumption were achieved when the exhaust opening was located at the ceiling level (rear-middle-level). Heidarinejad et al. [11] looked into the influence of return opening heights on thermal comfort, energy savings and indoor air quality in a room served by an underfloor air distribution (UFAD) system. They found that reducing the height of the return opening to 1.3 m above floor level will help improve energy savings by up to 15.3% for the same level of thermal comfort. Ahmed et al. [19] examined five different locations of the exhaust diffuser in an office room. In their results, a 25% energy saving was achieved when the exhaust opening was positioned at ceiling level and combined with ceiling lamps. Fitzgerald and Woods [20] found that the height of the exhaust opening has a significant impact on indoor air stratification.

From previous studies, it is clear that the exhaust opening location has a significant impact on the thermal environment indoors and on energy saving. In order to evaluate the performance of any new ventilation system, exhaust outlet location should be considered carefully. The current authors proposed a new ventilation system called the Local Exhaust Ventilation for Office rooms (LEVO), which provides a localised but comfortable environment for the

occupants whilst realising a low energy consumption [21]. Further investigation is required to select the best height of the exhaust opening for the LEVO, which may have a significant impact on the local thermal comfort and energy savings provided by the proposed system. Therefore, in this study, the performance of the new system was assessed using three different heights for the exhaust opening, the results of which were compared with a room where this system was not used. The indoor contaminants in an office room arise from office table equipment and by occupants' activities, and may contain noxious chemical substances [22, 23]. The quality of the enhanced air in the tested room using the LEVO system was assessed using two pollutant sources positioned at the workstations in front of each occupant to simulate contaminants coming from office equipment and occupants' activities.

2 Background to the investigated cases

The new LEVO air distribution system aims to enhance energy saving and improve the local thermal environment in the regions around the occupants by controlling the heat emitted from the room heat sources and contaminant distribution. The concept of combining the heat sources of the office workstation with an exhaust opening have been extensively investigated by the authors [19, 21, 24]. In this work, the LEVO system combines the reading lamps with the exhaust outlet in one unit, a combined system, and is located above the office workstation. The results show that the new local exhaust ventilation system can enhance energy saving significantly compared with an office without this system [21]. Further investigation is required to show the impact of the combined system's height on the local thermal environment with regards to thermal comfort, inhaled air quality and energy saving. Therefore, a comparison study was performed to show the impact on the energy saving and the indoor thermal comfort with and without the LEVO system. In the LEV system concept, the exhaust opening should not be away from the contaminant sources [12, 25-27]. Since this investigation aimed to provide a

local and comfortable thermal environment for the occupants by employing the developed LEVO system, the exhaust opening locations in relation to the room heat sources should be considered carefully. Therefore, three different heights, near the room heat sources and contaminant sources, of the combined system were investigated using numerical methods to find the influence of the height of the combined system on LEVO system performance (see Table 1). In this study a full-scale computational domain representing a typical office room with dimensions of 4.0 m long, 2.7 m high and 3.0 m wide was employed in the simulation.

Two occupants, two computer cases, two monitors, and two lamps were used to simulate the heat flux from the office room equipment. The heat flux from each heat source is presented in Table 2. Two sources of contaminant were used in this investigation to simulate the contaminants that might be emitted by the occupants' activities and office equipment. Particles of 0.7 μm diameter and a density of 912 kg/m^3 were used in this study. This kind of particle belongs to particles in the accumulation mode, 0.1-2.0 μm, such as those found in building dust and smoke. Recently, DV has attracted more attention worldwide due to its ability to improve the indoor air quality (IAQ) and provide a comfortable environment in the room [28-30]. For this reason, this system was used as the background ventilation system in this study. A supply DV outlet (1.0 m ×0.6 m) was positioned on the side wall at floor level. This position was selected to show the impact of using the new system on the local thermal environment for the occupant who is located slightly away from the DV supply diffuser in comparison with the one in front of the air diffuser supply. The return opening (0.08 m × 1.00 m) was located 1.3 m from floor level (see Fig.1 a). For case 1, the reference case, the exhaust opening was located at ceiling level on the side wall (see Fig. 1a). For all case studies, the room temperature was set to 24°C. Many monitoring points were used in different locations within the room domain and near the return outlet to make sure that the room reached the set temperature. In order to improve the occupants' productivity and the quality of the inhaled air, a high ventilation rate was recommended [31].

Therefore, in this study the supply air velocity was set at 0.14 m/s. In addition, since this study aimed to improve the indoor thermal comfort for occupants in summer, the supply air temperature of 19°C was selected for all the investigated cases. 35% of the supplied air was recirculated from the return opening, whilst the rest of the air was extracted from the proposed LEVO system at three different heights (see Table 1).

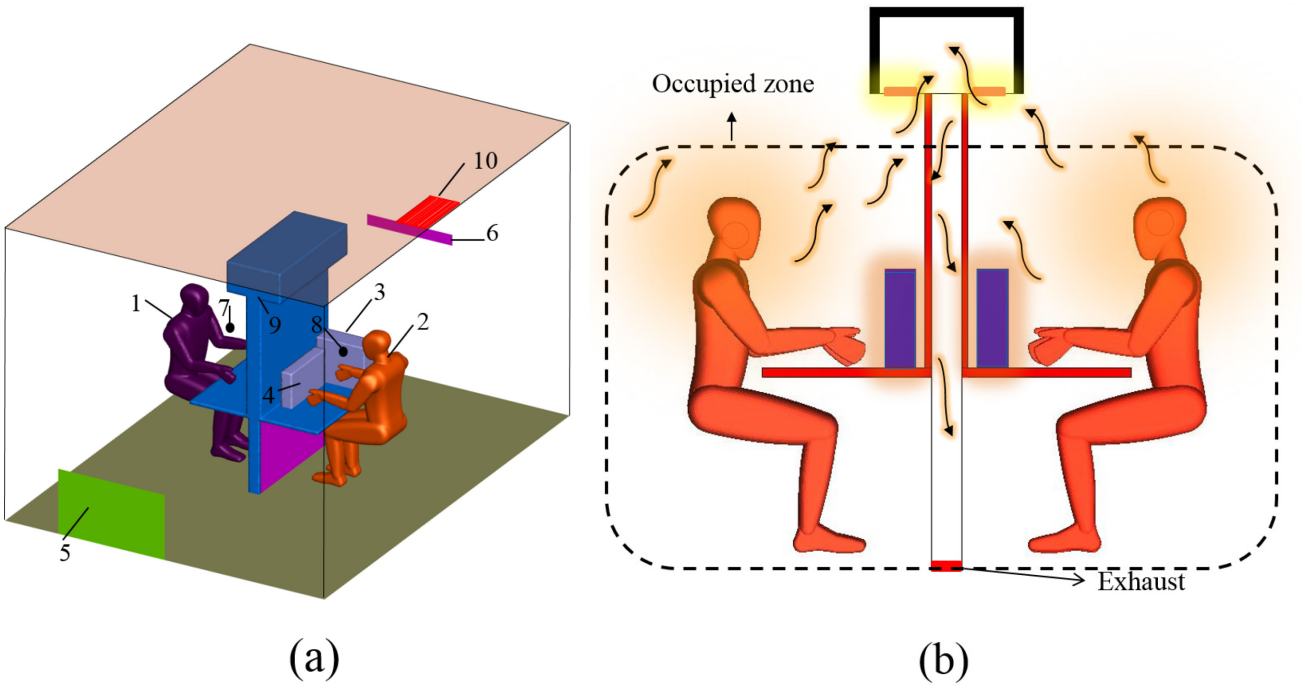

Fig.1. (a) Configuration of the simulated room: 1 - occupant 1, 2 - occupant 2, 3 - PC case, 4 - PC monitor, 5 - DV inlet, 6 - return inlet, 7 - contaminant source 1, 8 - contaminant source 2 and 9 - combined exhaust opening; 10 - exhaust location for case 1; (b) The LEVO system operation and flow direction.

Table 1 Case studies.

Case study	Heights of the combined system from floor level
Case 1	Reference case (without LEVO system)
Case 2	1.4 m
Case 3	1.6 m
Case 4	2.0 m

Table 2

Cooling load for the simulated office room.

Internal heat sources.	Cooling load
Occupants	60×2 (W)
PC case	60×2 (W)
PC monitor	70×2 (W)
Lamps	24×2 (W)
Bounded walls, ceiling and floor	Adiabatic wall
Total	428 (W)

3 CFD method

3.1 Mesh generation and mesh test

Due to the complexity of the investigated case, a tetrahedral unstructured mesh was used to generate the mesh system in the room domain using the ANSYS ICEM CFD software. The mesh density in the room domain was distributed with considerable care: a fine mesh was used in regions where high temperature gradients and velocities were expected, such as the regions around the occupants and other room heat sources and equipment, whilst a coarser mesh was generated in the regions slightly more distal from regions of interest.

The transition between the fine and coarser mesh was devised carefully to avoid any sudden coarseness that might otherwise cause problems during the simulation. For accurate predictions in the boundary layer region around the occupants and room heat sources, and to satisfy the y^+ values requirement, an inflation boundary layer was created using five layers of prism mesh

with a 1.2 growth rate (see Fig. 2). The thickness of the first layer was 1.5 mm and the y^+ values were $0.7 \leq y^+ \leq 4.5$. A grid test was performed to select the best mesh size and to make sure that the selected mesh was fine enough to gain accurate simulation results without introducing mesh artefacts. Depending on the grid test mesh, the total number of the mesh was 2,753,932, which would remain the mesh size for all further simulations.

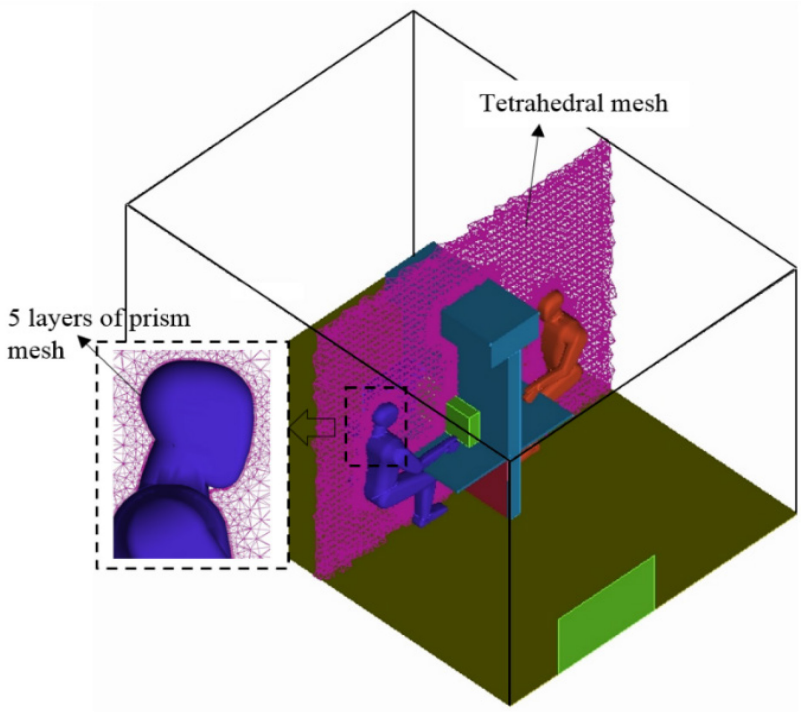

Fig. 2. Inflation boundary layer around the human body.

3.2 Air flow simulation models

In order to predict the indoor thermal environment and contaminant distribution accurately, a good simulation model needed to be selected. The two–equation renormalized group (RNG) $k-\varepsilon$ turbulence model was adopted to simulate the air flow and temperature distribution indoors. This model has the ability to predict the indoor air flow and contaminant

distribution with high accuracy [32-35]. The RNG $k-\varepsilon$ turbulence model can be written as follows [36]:

$$\frac{\partial(\rho k)}{\partial t}+\frac{\partial(\rho k u_i)}{\partial x_i}=\frac{\partial}{\partial x_j}\left[\left(\mu+\frac{\mu_t}{\sigma_k}\right)\frac{\partial k}{\partial x_j}\right]+P_k+\rho\varepsilon \quad (1)$$

$$\frac{\partial(\rho \varepsilon)}{\partial t}+\frac{\partial(\rho \varepsilon u_i)}{\partial x_i}=\frac{\partial}{\partial x_j}\left[\left(\mu+\frac{\mu_t}{\sigma_\varepsilon}\right)\frac{\partial \varepsilon}{\partial x_j}\right]+C_{1\varepsilon}\frac{\varepsilon}{k}P_k+C_{2\varepsilon}^{*}\rho\frac{\varepsilon^2}{k} \quad (2)$$

where

- $C_{2\varepsilon}^{*}=C_{2\varepsilon}+\left(C_\mu\eta^3(1-\eta/\eta o)\right)/1+\beta\eta^3$ with $\eta=(Sk/\varepsilon)$ and $S=\sqrt{2S_{ij}S_{ij}}$,

The values of the constants used in this model are given below:

- $C_\mu=0.0845,\ \sigma_k=0.7194,\ \sigma_\varepsilon=0.7194,\ C_{\varepsilon1}=1.42,\ C_{\varepsilon2}=1.68,\ \eta o=4.38$ and β =0.012.

The commercial software ANSYS Fluent was used in this study to evaluate the performance of the LEVO system in the simulated office space. The enhanced wall treatment is adopted to solve the boundary layer in the regions near the wall with a reasonable value of y^+. The Boussinesq assumption was employed to simulate the buoyancy effect due to the temperature variations in the simulation. Pressure and velocity field coupling was treated using the SIMPLE algorithm. The Second order-upwind discretisation scheme was selected to solve all the terms in the above equations except pressure, which is itself solved using PRESTO!. The discrete ordinates (DO) model [37] was used to simulate the radiation heat transfer of the room's internal heat sources. The numerical methods and boundary condition details used for this study are summarized in Table 3.

Table 3

Details of numerical methods and boundary conditions.

Turbulence model	Renormalized group RNG k − ε turbulence model.
Radiation model	Discrete ordinates (DO) radiation model.
Numerical schemes	For pressure, staggered third order scheme PRESTO!; for other terms, upwind second order; SIMPLE algorithm.
Ceiling, floor, tables and bounded walls	Adiabatic wall
Supply air	Velocity inlet (0.14 m/s), supply temperature (19 °C)
Exhaust	Pressure –outlet
Occupants	Uniform heat flux 60 W×2
PC case	Uniform heat flux 60 W ×2
PC monitor	Uniform heat flux 70 W ×2
Lamps	Uniform heat flux 24 W ×2

3.2.1 Discrete Phase Modelling (DPM)

The Eulerian-Eulerian or the Eulerian-Lagrangian approach is considered one of the most powerful CFD tools and is widely used to simulate particle distributions indoors [38]. In this investigation, the particles' trajectories through the continuous phase (fluid phase) was tracked and calculated using an Eulerian-Lagrangian method, the so-called Discrete Phase Model (DPM). In this approach, the continuous phase was simulated using Eulerian methods and the discrete phase (airborne particles) was simulated using the Lagrangian approach. The Reynolds-averaged Navier-Stokes equations were adopted to solve for the fluid phase, which is treated as a continuum, while the discrete phase was calculated by tracking individual particle trajectories through the flow field. On the assumption that the volume fraction was sufficiently small, the one-way coupling assumption was adopted in this study. In this assumption, particles are influenced by the drag and turbulence of the airflow, but the particles themselves have no effect on the fluid phase [39].

The particle size can be categorised in three ways: ultrafine (< 0.1 μm); accumulation (0.1-2.0 μm) and coarse (> 2 μm) [40]. The accumulation mode was adopted in this study to predict the contaminant concentration distribution in the occupied zone.

3.2.1.1 Particles tracking equations

The individual trajectories of each particle were calculated using the Lagrangian approach. By equating the inertia force of the particle to the external forces acting on it, the momentum equation can be written as below:

$$\frac{d\vec{u}_p}{dt} = F_D\left(\vec{u} - \vec{u}_p\right) + \frac{\vec{g}(\rho_p - \rho)}{\rho_p} + \vec{F}_a \tag{3}$$

The left-hand side of eq. (3) represents the inertial force per unit mass ($m\ s^{-2}$), while the first term on the right-hand side refers to drag forces per unit mass. The second term of eq. (3) represents the gravitational and buoyancy forces.

The additional forces (per unit mass) were added using $\vec{F}_a$, which may have an impact on particle transition. The main force acting on the particles is the drag, which follows the Stokes drag law:

$$\vec{F}_{drag} = F_D\left(\vec{u} - \vec{u}_p\right) = \frac{18\mu}{\rho_p d_p^2\, C_c}\left(\vec{u} - \vec{u}_p\right) \tag{4}$$

where C_c is the Cunningham correction factor, which can be calculated via the following equation:

$$C_c = 1 + \frac{2\lambda}{d_p}\left(1.257 + 0.4e^{-(1.1 d_p/2\lambda)}\right) \tag{5}$$

where λ is the molecular mean free path.

By comparing with the drag force, the Basset history, the pressure gradient and virtual mass had no strong influence on the particles. For this reason, these forces were neglected in this study.

The particle motion indoors is influenced by Brownian motion and Saffman lift forces, especially in the regions near the wall where the turbulent boundary layer works effectively [41], and these forces have a considerable role in the deposition process [42-44]. For this reason, the current investigation has taken these forces into account. The final form of trajectory equation becomes:

$$\frac{d\vec{u}_p}{dt} = F_D\left(\vec{u} - \vec{u}_p\right) + \frac{\vec{g}(\rho_p - \rho)}{\rho_p} + \vec{F}_b + \vec{F}_s \tag{6}$$

The local turbulence intensities have a significant impact on particle motion indoors. Therefore, the discrete random walk (DRW) method was adopted in this study to predict the stochastic velocity fluctuations in the turbulent airflow [45]. The final form of the fluctuating velocity components can be expressed as follow:

$$u_i' = \xi_i\sqrt{2k/3} \tag{7}$$

where u_i' represents the fluctuating velocity.

Due to the small volume fraction where the particles path was influenced by the flow field, and given that there is no influence of the particle on the flow field itself, the air flow field is calculated first, and then the particles are injected [46]. The ANSYS Fluent software was used to solve the air flow equations and Lagrangian trajectories of the particles' motions. However, in Fluent there is no direct way to calculate the particle concentration in the flow field. For this reason, the particle concentration was calculated using a user-defined function (UDF). The particle source in-cell (PSI-C) method was adopted by correlating the concentration with the trajectories for each computational cell, as shown below:

$$C = \frac{\dot{m} \sum_{i=1}^{n} dt(i,j)}{V_j} \quad (8)$$

Zhang and Chen [38] have looked at the Lagrangian model in terms of its accuracy and the stability. They found that the concentration calculations are statically stable when a sufficient number of trajectories are tracked in the fluid domain. Depending on their results, in the present study, adequate numbers of particle trajectories have been tracked in the flow field domain to gain an accurate and stable solution to the Lagrangian model.

3.2.1.2 Boundary conditions

At the inlets and exhaust outlet, the particles escape and their trajectories will terminate; the particles will then either attach to the solid outer surface of any solid object, or otherwise rebound from these surfaces. For the indoor air application, the particles intend to attach to the outer solid surface because they do not have enough energy to rebound, i.e., to overcome adhesion [47]. In order to avoid the poor predicted results, the mesh near the walls need to be sufficiently fine. At the boundary layer region near the wall, the viscous sub-layer kinetic energy and the fluctuating velocity will increase, cause an increase in the number of collisions between the particles with the walls. Therefore, an inflation boundary layer was adopted in these regions to provide the required near-wall grid refinement and provide a more accurate prediction.

4 Validation work

4.1 Air velocity and temperature validation

In order to gain accurate and reasonable predicted results, the CFD model needs to be validated against experimental results. The experimental data for velocity and temperature distributions reported by Xu et al. [48] were used to validate the selected (RNG) $k-\varepsilon$ turbulence model to make sure that it was working well with the investigated case study. As

shown in Fig. 3 a and b, the experimental work was performed in a small room, 6.00 m long, 3.90 m wide, and 2.35 m high, and the internal heat sources included one computer and one occupant with heat fluxes of 40 W and 76 W, respectively.

The supply air flow rate was 43 m^3/h and the supply air temperature was 19°C. The comparison between the experimental and predicted results for the velocity profile and temperature distribution are shown in Figs. 4 and 5, respectively. From these figures, it is fair to say that the selected model can predict the indoor thermal environment efficiently. More information regarding experimental details can be found in the work of Xu et al. [48].

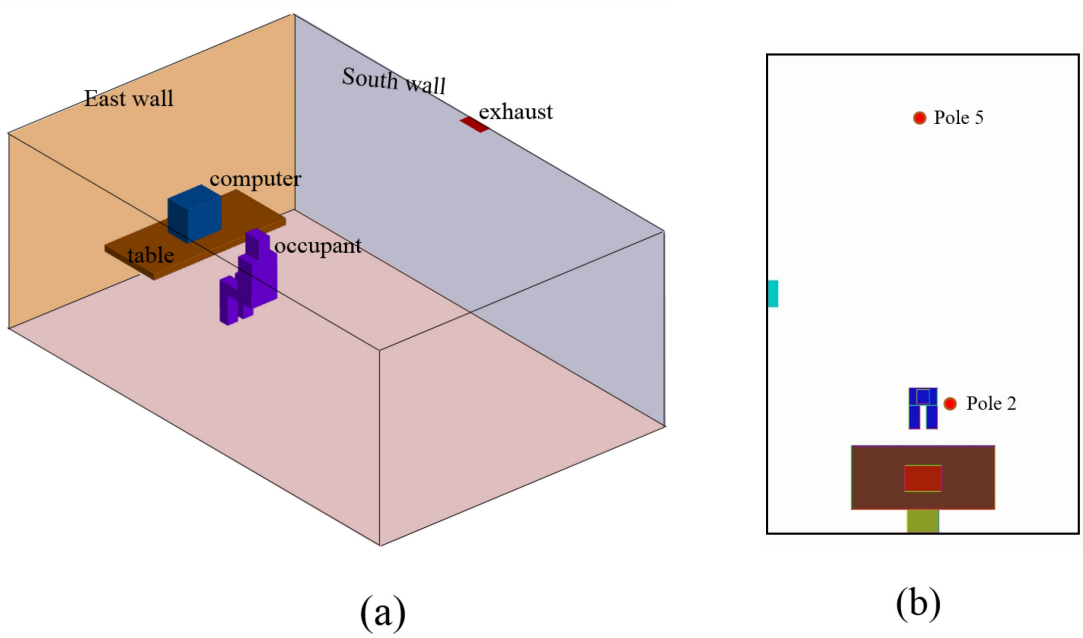

Fig. 3. (a) Schematic diagram of the experimental chamber for validation [48]; (b) The arrangement of the measured locations.

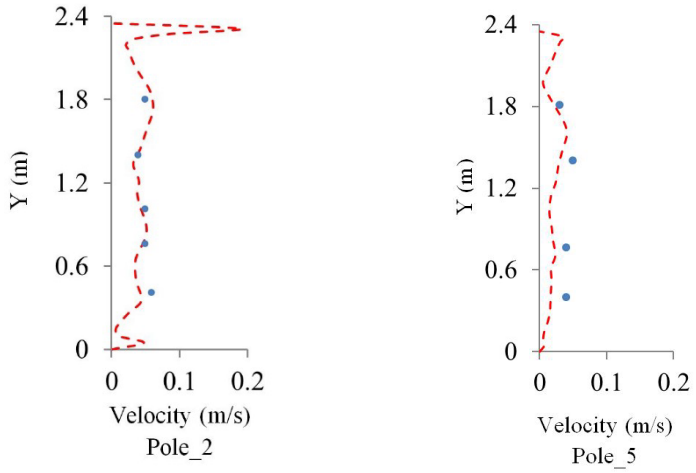

Fig. 4. Comparison of measured and simulated velocity profiles (circular symbols: experimental velocity [48]; dashed line: simulated velocity).

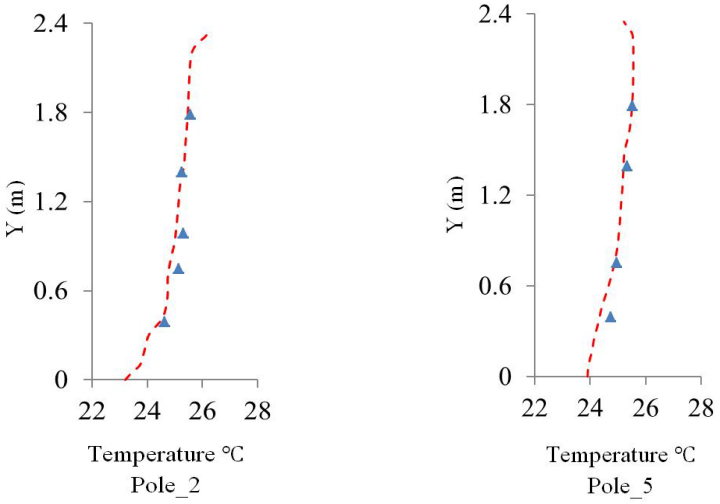

Fig. 5. Comparison of measured and simulated temperature profiles (triangular symbols: experimental temperature [48]; dashed line: simulated temperature).

4.2 Particle distribution validation

The experimental data of Chen et al. [49] are used in this study to validate the Lagrangian particle-tracking model. The dimensions of the experimental chamber were 0.8 m × 0.4 m × 0.4 m (see Fig. 6). The inlet velocity was 0.225 m/sec. The diameter of the particles and their density were 10 μ m and 1400 $\mathrm{kg/m^3}$, respectively. The concentration of the particles is normalized by the inlet concentration. The normalised particle concentration was calculated at three different positions. As presented in Fig. 7, a good agreement was found by comparing the predicted results with experimental results, which confirms the ability of this model to accurately determine particle distributions. More information regarding this validation can be found in reference [49].

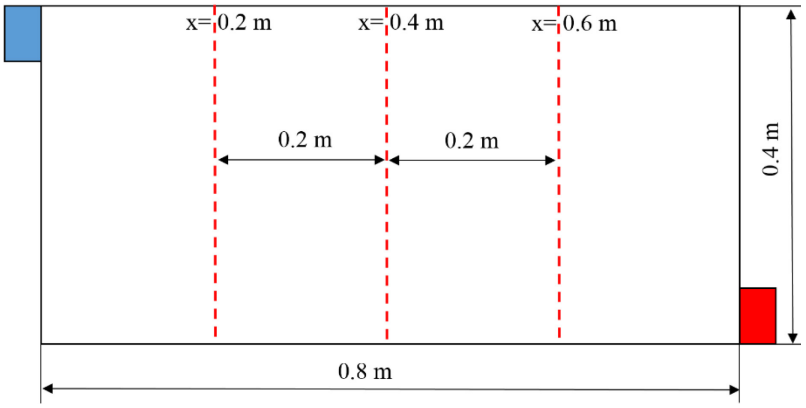

Fig. 6. Schematic diagram of ventilated chamber for the validation of Lagrangian particle-tracking [49].

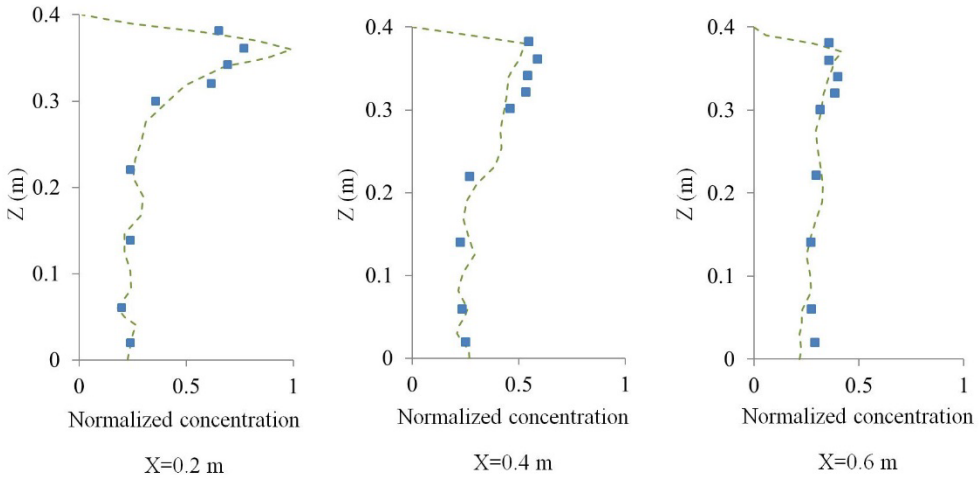

Fig. 7. Comparison between the normalised particle concentration and experimental results [49] at three different locations x = 0.2, 0.4 and 0.6 (square symbols: experimental data [49]; dashed line: predicted normalized particle concentration).

5 Results and discussion

5.1 Temperature distribution near foot zone

In DV system, the supply diffuser is normally located at the floor level. In this system, fresh, cooled air is supplied at a low velocity [50]. The DV system is widely used in office spaces because of its ability to provide a healthy and comfortable environment [51]. However, a draft risk due to the temperature difference between the head and feet levels, as well as contaminant distribution, are considered to be the main drawbacks of this type of ventilation system. Therefore, this study aimed to overcome the main disadvantages of DV systems by extracting the warmed and contaminated air from the occupied zone and direct it towards foot level. This process will help to reduce the temperature differences between foot and head level [21]. Three different heights for the LEVO system were investigated (see Table 1) and compared with a reference case.

As shown in Fig. 8 a, three monitoring points, points 1, 2 and 3, in the foot zone are used to evaluate the air temperature in various regions for each case study and for occupant_1 and occupant_2. Fig. 8 b and c show the calculated air temperatures for all monitoring points. From these figures, it is clear that in case 1, when the room does not use the proposed system, the air temperatures at the three monitoring points are slightly lower than the temperatures in the other case studies, case 2, 3 and 4. This was because the warm air extracted by the LEVO will help to increase the air temperature in the foot zone slightly. In addition, by changing the height of the exhaust opening, there is no noticeable difference in the air temperature values for case 2, 3 and 4 for occupant-1, though for occupant-2, the air temperature in case 3 is slight higher than in the other case studies. This was due to the position of occupant 2 being slightly further away from the inlet opening. In addition, at this height a large amount of the warmed air was extracted directly from the occupant zone and directed towards the foot zone, which will subsequently increase the air temperature in these regions compared with the other cases.

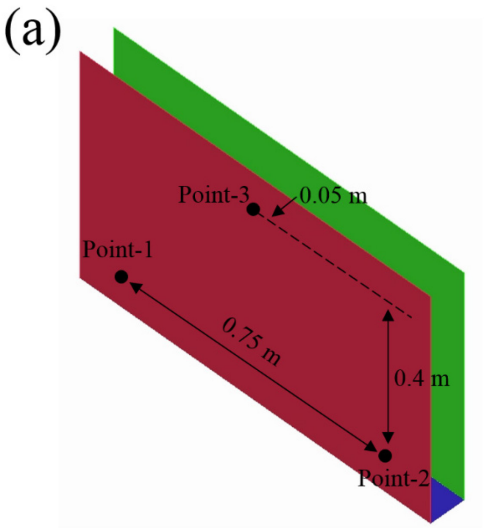

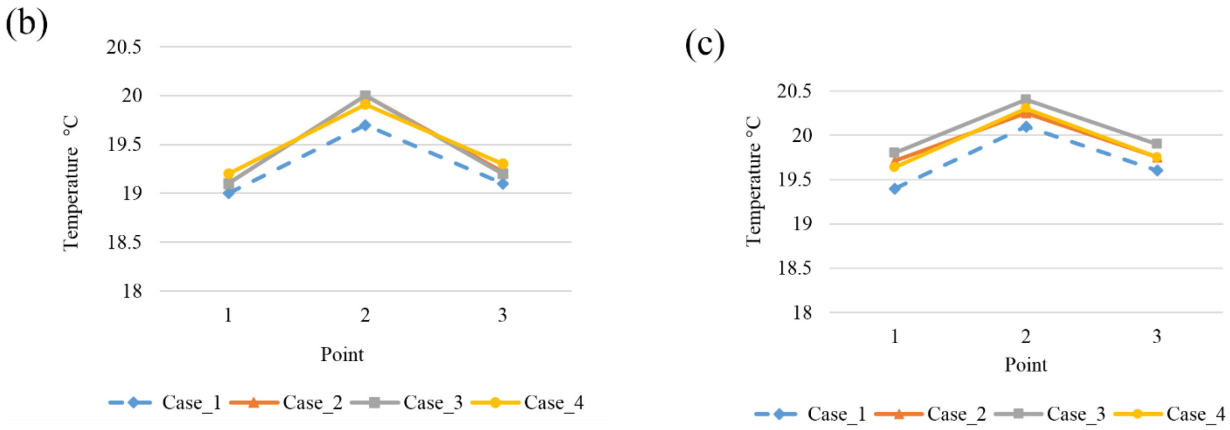

Fig. 8. (a) Three monitoring points, point 1, 2 and 3, for each case study and (b) and (c) temperature distribution (℃) of the near foot zone for occupant_1 and occupant_2 respectively.

5.2 Occupants thermal discomfort evaluation

The temperature difference between the head and foot level should not be more than 3℃ [52]. In this study, human thermal discomfort was evaluated for all case studies. Fig. 9 a shows the locations of the four monitoring points (points 1, 2, 3 and 4), two being in the region of each occupant. Fig. 9 b shows the results of the vertical temperature distribution in all case studies. From these results, it is clear that using the proposed LEVO system, case 2, 3 and 4 enhanced the temperature profile in the vertical direction in all positions compared with case 1 (the room in which the system was not used). In cases 2 and 4, there is no big difference in the temperature differences values ($\Delta T_{head-foot}$) across all measurement points. Although the thermal comfort was satisfactory, with $\Delta T_{head-foot}$ < 3°C in all cases when the new LEVO system was used, case 3 seemed to show a relatively high temperature difference ($\Delta T_{head-foot}$) compared with cases 2 and 4. However, in this case, case 3, the temperature difference ($\Delta T_{head-foot}$) still in the acceptance range. The local extraction of the warmed air generated will help to enhance the temperature homogeneity between the upper and lower parts of the room. Fig.10 shows the temperature and velocity distribution for all case studies. From these figures, the upper part of the room in case 1 was warmer than the other case studies, and the

velocity distribution was also more turbulent. This was considerable enough that it might cause human discomfort. In cases 2, 3 and 4 when the proposed LEVO system was used, more homogenous temperature and velocity distributions were found in all room domains. In case 3, the temperature and velocity distribution are more homogeneous than in cases 2 and 4. In cases 2 and 4, the temperature and velocity distribution will be less homogeneous than in case 3. This was due to the fact that case 3 did not allow to the generated thermal plumes to keep developing and thus disturb the flow in the rest of the room domain. The LEVO system decreased the temperature in the upper part of the room by extracting most of the generated heat. This will create different air stratification for each case. In case 4, the large amount heat generated in the occupied zone may escape before its extraction from the LEVO system, compared to the heat that may be extracted from the upper part of the room at 2 m. For this reason, the combined system in case 4 seems slightly less warm than in cases 2 and 3 (see Fig. 10).

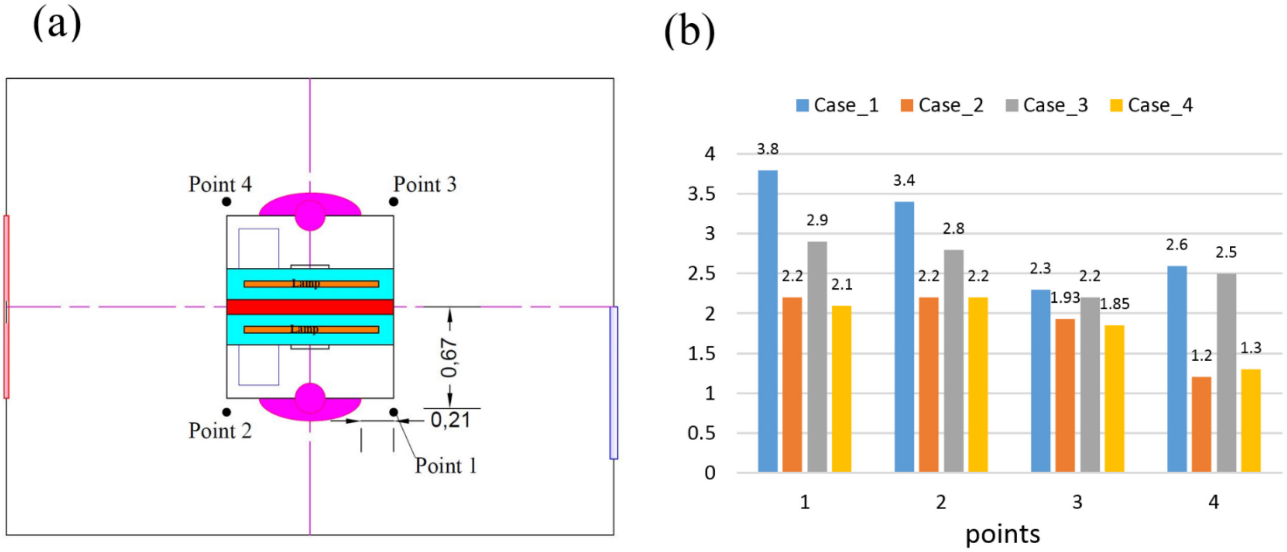

Fig. 9. (a) Monitoring points; (b) Temperature gradient in the vertical direction for each case study at four measuring points.

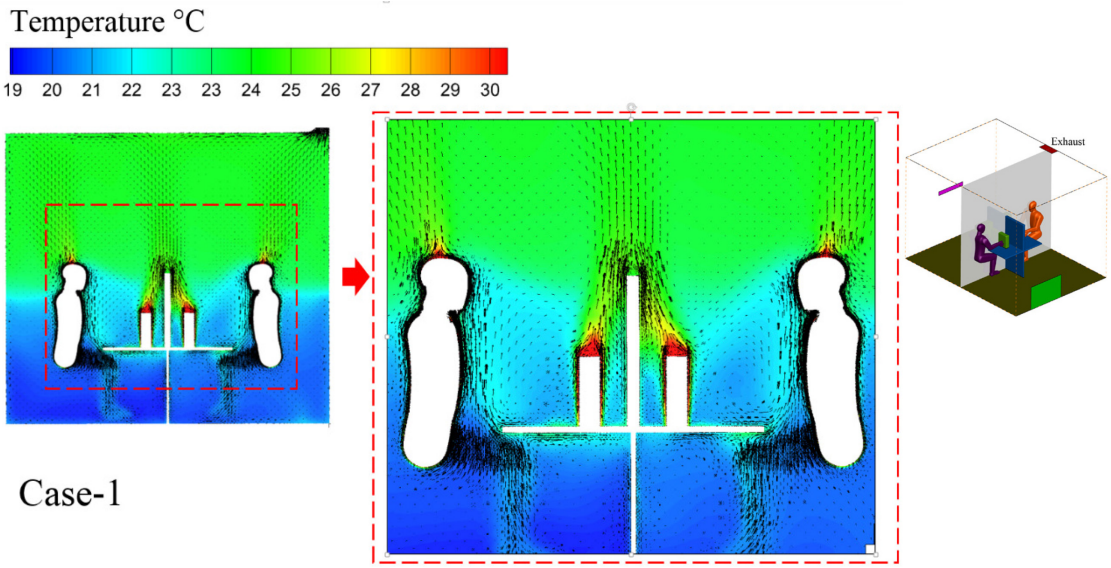
Temperature °C
19 20 21 22 23 23 24 25 26 27 28 29 30
Exhaust
Case-1

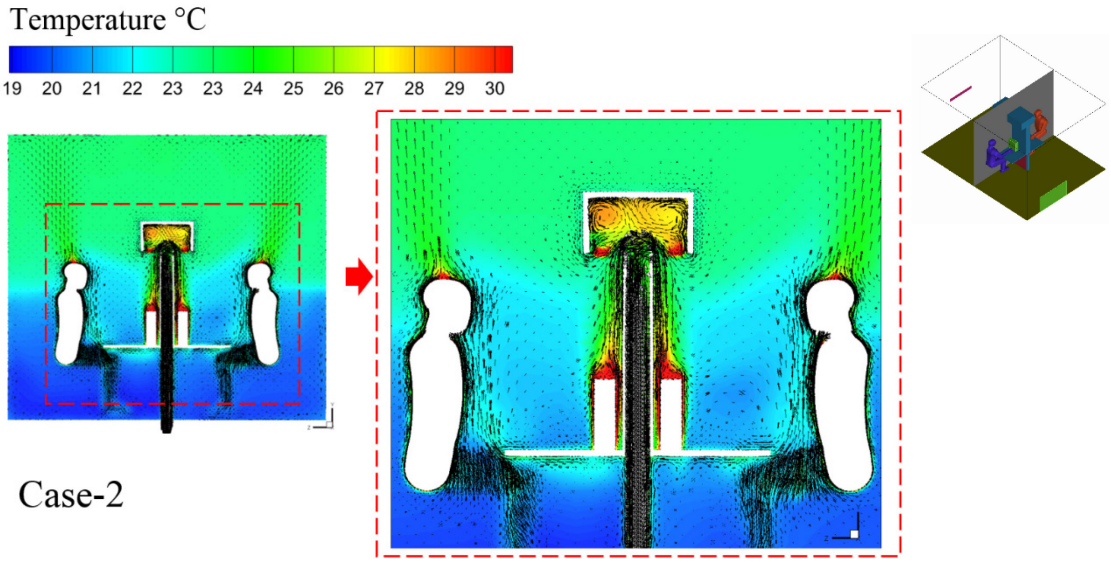
Temperature °C
19 20 21 22 23 23 24 25 26 27 28 29 30
Case-2

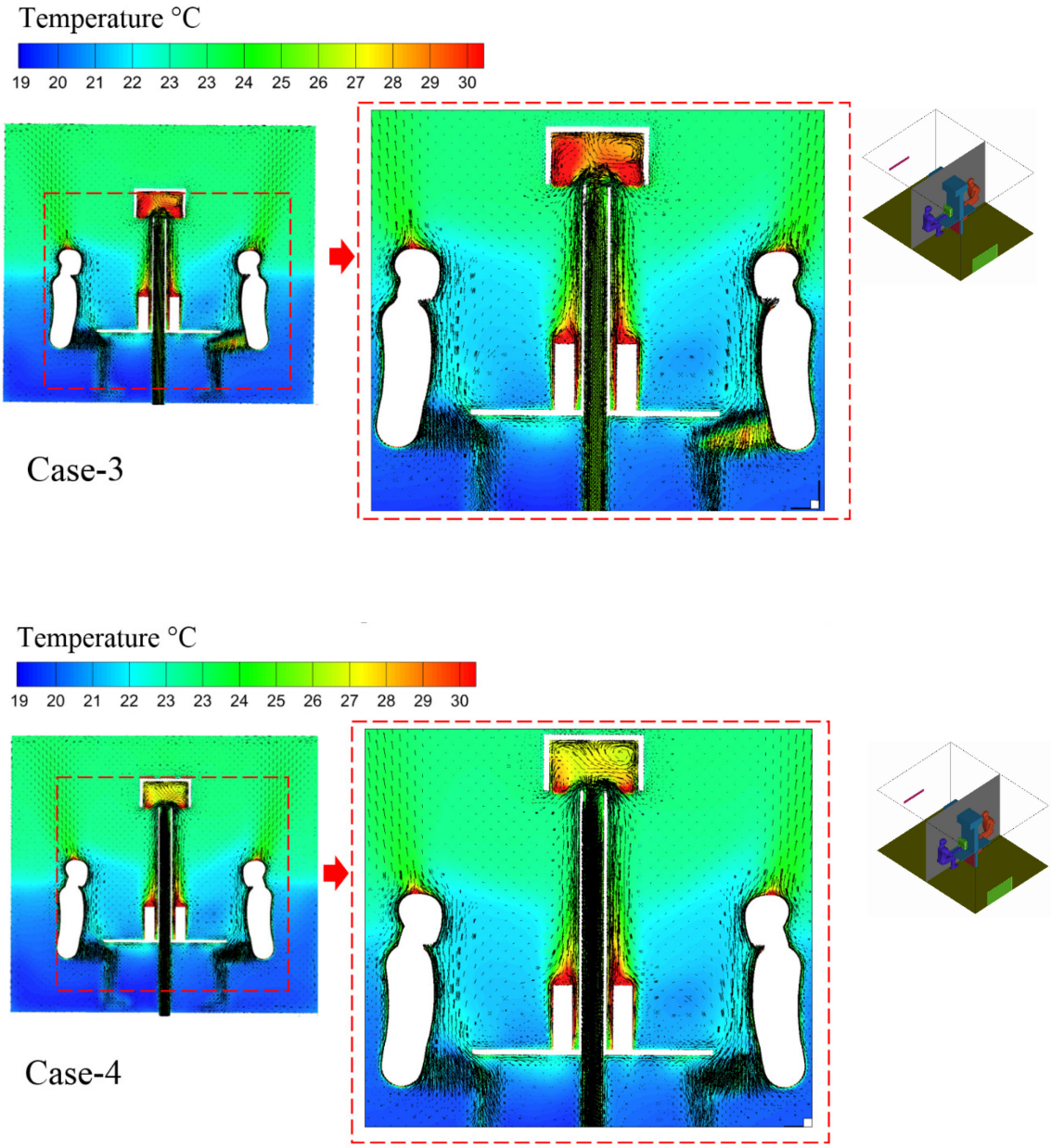

Fig. 10. Temperature and velocity distribution in the mid plan (x = 2 m) for each case study.

5.3 Draught risk evaluation

Draught is an undesired local overcooling of the occupants caused by air flow [53], and is considered as one of the most common and significant problems in indoor spaces. This problem occurs when the fresh and cool air is supplied directly to the occupied zone at floor level, as in DV systems [54]. In any ventilation system, the risk of draughts is a major issue that needs to be evaluated to ensure the ability of the ventilation system to provide acceptable

thermal comfort. Draught risk can be measured by the percentage of dissatisfied people due to the draught (PD), which should ideally not exceed 20 % (the maximum allowable value) [55]. Therefore, in any ventilation system, the PD values, particularly in the occupied zone, should be considered carefully. In this study, the PD analysis was carried out for all case studies for each occupant. The PD evaluation was performed at the ankle level (0.1 m from floor). This level 'contains' the most important parts of the occupants' bodies in terms of feeling the sensation of draught, and consequently the highest draught risk has been identified as being at this level[56-58].

In this study, PD was evaluated by using Fanger's equation [53]:

$$\mathrm{PD} = (34 - T)(u - 0.05)^{0.62}\,(3.14 + 0.37\,u\,T_u) \tag{9}$$

for $u < 0.05$, use $u = 0.05$ m/sec

for $\mathrm{PD} > 100\%$, use $\mathrm{PD} = 100\%$

where T and u are the air temperature and mean air velocity, respectively.

T_u is the air turbulent intensity, which is determined by:

$$T_u = 100\frac{(2k)^{0.5}}{u} \tag{10}$$

where k is the turbulent kinetic energy, which itself is defined as:

$$k = 1.5\,(u\,T_u)^2 \tag{11}$$

Fig. 11 shows the results of the PD evaluation in all case studies. From these results, it is clear that there is no significant difference in the PD for either occupant in all case studies. However, the draught risk was slightly increased when using the proposed LEVO system, as in case 2, 3 and 4 when compared with case 1 (No LEVO system was used). This was because the local extraction of air can increase the air movement in the occupant zone, consequently increasing the draught risk. Furthermore, for all case studies, the PD values for occupant -1 were higher than for occupant -2. This was because the location of occupant -1 was directly in

front of the DV supply diffuser. This can result in direct 'contact' between occupant -1 and the supply air (supply velocity and temperature). All in all, the draught risk in all case studies fell within the acceptance range, and did not exceed the maximum allowable value of 20% [55].

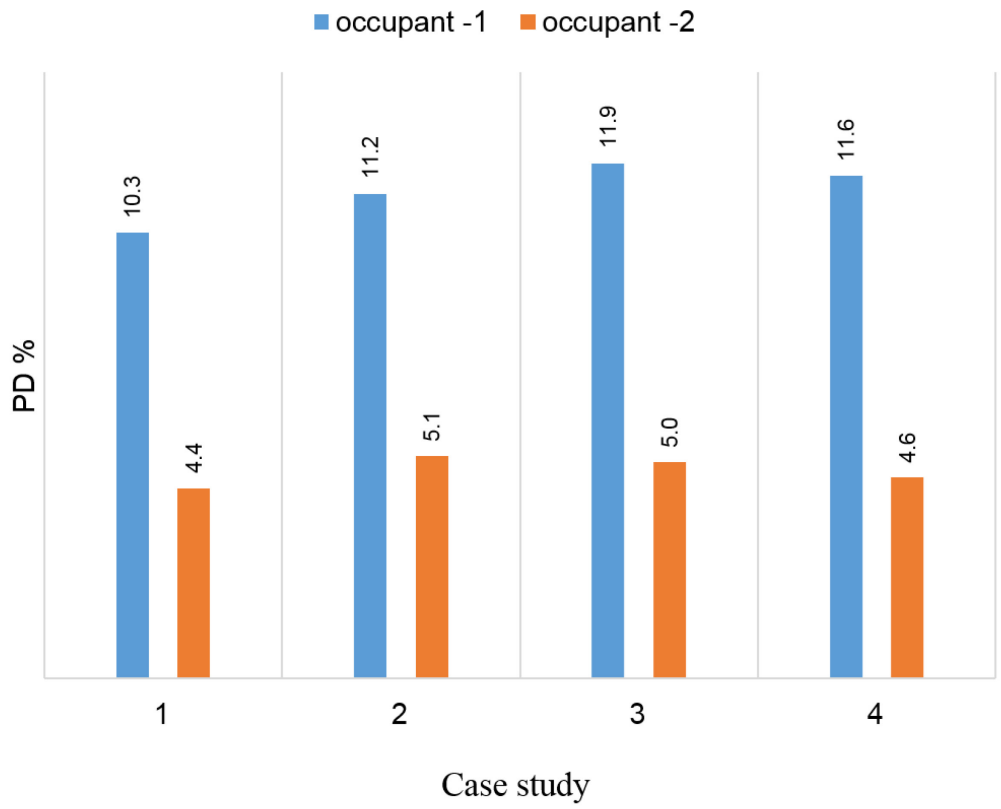

Fig. 11. Comparison of the PD for both occupants in each case study.

5.4 Energy saving evaluation

For any ventilation system, the energy saving evaluation is considered one of the principle evaluation indices. In this study, the energy saving was evaluated for all cases studies. Cheng et al. [10] proposed a new method by which to evaluate the amount of energy saving by calculating the reduction in cooling coil load depending on the CFD results. This method is widely used in energy saving evaluation in the majority of ventilation systems [9-11, 19, 59]. The cooling coil load calculation in the STRAD system is different to the calculation for the mixing ventilation system (MV):

$$Q_{coil-STRAD} = Q_{coil-MV} - c_p \times \dot{m}_e \times (T_e - T_{set}) \quad (12)$$

$$Q_{coil-MV} = Q_{space} + Q_{vent} \quad (13)$$

where T_{set} is the set room temperature, which is the same for all case studies, and T_e is the exhaust air temperature. $\dot{m}_e$ is the exhaust air mass flow rate. The reduction of cooling coil load is expressed in terms of $c_p \times \dot{m}_e \times (T_e - T_{set})$, which is used to assess the LEVO system's efficiency in terms of energy consumption.

The reduction in the cooling coil load and the associated energy savings are presented in Table 4. From these results, it is clear that the energy saving has improved significantly in the room using the LEVO system, cases 2, 3 and 4, as compared with the reference case. This is due to

Table 4
Energy saving for cooling coil for each case study.

	Case 1	Case 2	Case 3	Case 4
Exhaust air temperature $T_{exhaust}$ (℃)	24.3	25	25.4	25.1
Return air temperature T_{return} (℃)	23.1	22.4	22.3	22.4
ΔQ_{coil} (W)	21.7	70	96.5	75.8
$\Delta Q_{coil}/Q_{space}$ (%)	5.07	16.1	22.56	17.8

the fact that the local extraction of the warm air generated by the room's internal heat sources leads to an increase in the air temperature at the exhaust opening, consequently improving the potential energy saving [21]. In addition, case 3 was the best in terms of saving energy at about 22.56% improvement, compared with 5.07% in case 1, 16.1% in case 2 and 17.8 % in case 4. The reason here was that compared with cases 1, 2 and 4, case 3 extracted a large amount generated heat at this height of the LEVO system, as this height did not allow a large amount of warmed air to escape to the rest of the room air. Thus, to improve energy savings, an appropriate height for the LEVO system needs to be carefully selected. In the assessment of energy saving, other factors such as temperature profile distribution in the vertical direction and the air quality in the occupied zone should also be considered carefully.

5.5 The quality of indoor air in breathing and inhaled zones

A healthy and comfortable working environment are principle requirements in improving occupant productivity. For office spaces, the quality of the inhaled air plays a significant role in occupant productivity. Therefore, in any ventilation system, the quality of the indoor air, particularly in the occupied zone, should be considered carefully. In the office room, contaminants generally arise from both equipment and occupants. Thus, in this study, two contaminant sources were located to the front of each occupant were used to simulate the main sources of contaminant in office room (see Fig. 1 a). In this study, as shown in Fig. 12 a, the quality of the inhaled air is evaluated in region around each occupant's head. Furthermore, the quality of the indoor air in the breathing zone was also evaluated. The normalised contaminant concentration is defined as follows:

$$C_n = \frac{C_p}{C_e} \tag{14}$$

where C_n is the normalised concentration, and C_p and C_e are the contaminant concentrations in a specific zone and the exhaust opening, respectively.

Figs. 12 b and c show the normalised particle concentration in the breathing and inhaled zone, respectively, for each case study. From these figures, it is clear that a significant improvement in the quality of the indoor air in both inhaled and breathing zones was achieved in a room using the LEVO system, cases 2, 3 and 4, compared with the reference case. This was because a significant amount of the contaminants generated by the equipment and occupants' activities was extracted locally and directly via the LEVO system before it could disperse into the occupied zone [21]. By comparing case 3 with cases 2 and 4, it is clear that in case 3 a high contaminant concentration was observed compared with cases 2 and 4. This was because at this height, a certain amount of contaminant escaped and was dispersed directly into the inhaled air, which consequently increased the contaminant distribution concentration in the inhaled zone. However, in this case, case 3, the room air quality still in acceptance range. From

these results, it can be concluded that the quality of the indoor air was influenced by the height of the combined exhaust opening in the room that used the LEVO system. Therefore, the quality of the indoor air in the breathing zone was enhanced significantly by selecting a suitable height for the combined system.

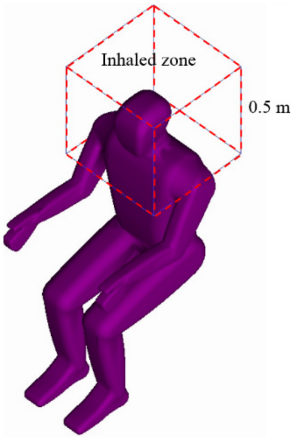

(a)

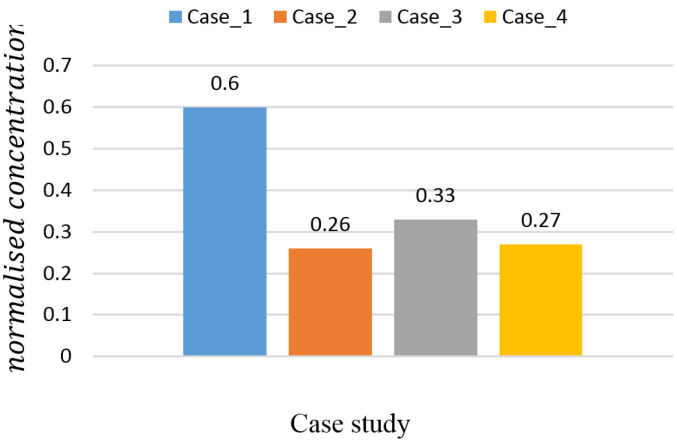

(b)

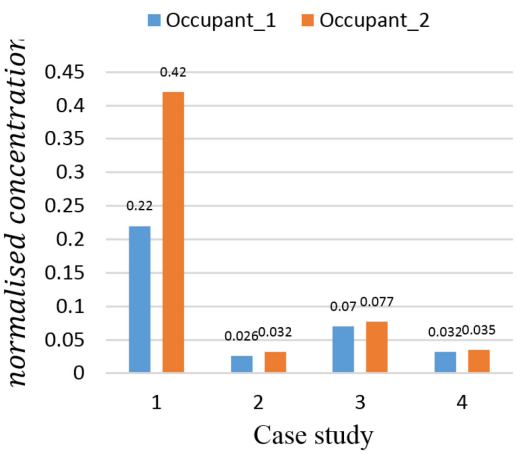

(c)

Fig. 12. Comparison of the quality of indoor air for each case study; (a) inhaled zone; (b) contaminant concentration at breathing level; (c) the inhaled air quality for both occupants.

6 Conclusion

The investigation of the height impact for the proposed LEVO system was performed numerically in this study. Three different heights (1.4 m, 1.6 m and 2.0 m) for the combined system were used to evaluate the performance of the LEVO system in the office spaces. From the results of this investigation, it can be concluded that:

- Four case studies have been successfully carried out numerically using the general purpose CFD code Fluent with the RNG $k-\varepsilon$ turbulence model and the Lagrangian discrete phase tracking model.
- The performance of the LEVO system is highly influenced by the exhaust combined opening heights. Therefore, in order to gain optimal performance from the LEVO system, height selection should be considered carefully.
- For the studied LEVO system cases, the thermal comfort and indoor air quality in cases 2 (1.4 m) and 4 (2.0 m) were slightly better than those in case 3 (1.6 m). However, a significant amount of energy saving of 22.56% and acceptable air quality with a good thermal comfort were achieved in case 3. Since the aim of this study was to improve energy savings and provide acceptable quality inhaled air and good thermal comfort, case 3 was considered to be the best height at which optimal performance could be gained from the LEVO system.
- The draught risk evaluation was conducted for all case studies, and the relevant PD values fell comfortably within the required range, which provides further support to the LEVO system.

7 Acknowledgements

The authors would like to thank the Ministry of Higher Education and Scientific Research of Iraq for the financial support of the project.

References

[1] Seppanen O. Ventilation rates and health. ASHRAE journal. 2002;44:56.

[2] Seppänen OA, Fisk W. Some quantitative relations between indoor environmental quality and work performance or health. Hvac&R Research. 2006;12:957-73.

[3] Wyon DP, Wargocki P. How indoor environment affects performance. thought. 2013;3:6.

[4] Calay RK, Wang WC. A hybrid energy efficient building ventilation system. Applied Thermal Engineering. 2013;57:7-13.

[5] Chemisana D, López-Villada J, Coronas A, Rosell JI, Lodi C. Building integration of concentrating systems for solar cooling applications. Applied Thermal Engineering. 2013;50:1472-9.

[6] Fong K, Chow TT, Li C, Lin Z, Chan L. Effect of neutral temperature on energy saving of centralized air-conditioning systems in subtropical Hong Kong. Applied Thermal Engineering. 2010;30:1659-65.

[7] Guo Y, Zhang G, Zhou J, Wu J, Shen W. A techno-economic comparison of a direct expansion ground-source and a secondary loop ground-coupled heat pump system for cooling in a residential building. Applied Thermal Engineering. 2012;35:29-39.

[8] Hawendi S, Gao S. Impact of an external boundary wall on indoor flow field and natural cross-ventilation in an isolated family house using numerical simulations. Journal of Building Engineering. 2017;10:109-23.

[9] Cheng Y, Niu J, Du Z, Lei Y. Investigation on the thermal comfort and energy efficiency of stratified air distribution systems. Energy for Sustainable Development. 2015;28:1-9.

[10] Cheng Y, Niu J, Liu X, Gao N. Experimental and numerical investigations on stratified air distribution systems with special configuration: Thermal comfort and energy saving. Energy and Buildings. 2013;64:154-61.

[11] Heidarinejad G, Fathollahzadeh MH, Pasdarshahri H. Effects of return air vent height on energy consumption, thermal comfort conditions and indoor air quality in an under floor air distribution system. Energy and Buildings. 2015;97:155-61.

[12] Junjing Y, Sekhar C, Cheong D, Raphael B. Performance evaluation of an integrated Personalized Ventilation–Personalized Exhaust system in conjunction with two background ventilation systems. Building and Environment. 2014;78:103-10.

[13] Halvonová B, Melikov AK. Performance of ductless personalized ventilation in conjunction with displacement ventilation: impact of workstations layout and partitions. HVAC&R Research. 2010;16:75-94.

[14] Kanaan M, Ghaddar N, Ghali K. Quality of inhaled air in displacement ventilation systems assisted by personalized ventilation. HVAC&R Research. 2012;18:500-14.

[15] Yang J, Sekhar C, Wai DCK, Raphael B. Computational fluid dynamics study and evaluation of different personalized exhaust devices. HVAC&R Research. 2013;19:934-46.

[16] Nielsen PV, Li Y, Buus M, Winther FV. Risk of cross-infection in a hospital ward with downward ventilation. Building and Environment. 2010;45:2008-14.

[17] Cheong K, Phua S. Development of ventilation design strategy for effective removal of pollutant in the isolation room of a hospital. Building and Environment. 2006;41:1161-70.

[18] Fong M, Hanby V, Greenough R, Lin Z, Cheng Y. Acceptance of thermal conditions and energy use of three ventilation strategies with six exhaust configurations for the classroom. Building and Environment. 2015;94:606-19.

[19] Ahmed AQ, Gao S, Kareem AK. A numerical study on the effects of exhaust locations on energy consumption and thermal environment in an office room served by displacement ventilation. Energy Conversion and Management. 2016;117:74-85.

[20] Fitzgerald SD, Woods AW. Natural ventilation of a room with vents at multiple levels. Building and Environment. 2004;39:505-21.

[21] Ahmed AQ, Gao S, Kareem AK. Energy saving and indoor thermal comfort evaluation using a novel local exhaust ventilation system for office rooms. Applied Thermal Engineering. 2017;110:821-34.

[22] Licina D, Melikov A, Pantelic J, Sekhar C, Tham KW. Human convection flow in spaces with and without ventilation: personal exposure to floor-released particles and cough-released droplets. Indoor air. 2015.

[23] Pereira M, Graudenz G, Tribess A, Morawska L. Determination of particle concentration in the breathing zone for four different types of office ventilation systems. Building and Environment. 2009;44:904-11.

[24] Ahmed AQ, Gao S. Thermal Comfort and Energy Saving Evaluation of a Combined System in an Office Room Using Displacement Ventilation. World Academy of Science, Engineering and Technology, International Journal of Mechanical, Aerospace, Industrial, Mechatronic and Manufacturing Engineering. 2015;9:1078-83.

[25] Ho SH, Rosario L, Rahman MM. Three-dimensional analysis for hospital operating room thermal comfort and contaminant removal. Applied Thermal Engineering. 2009;29:2080-92.

[26] Li X, Niu J, Gao N. Co-occupant's exposure to exhaled pollutants with two types of personalized ventilation strategies under mixing and displacement ventilation systems. Indoor air. 2013;23:162-71.

[27] Qian H, Li Y, Nielsen PV, Hyldgaard CE. Dispersion of exhalation pollutants in a two-bed hospital ward with a downward ventilation system. Building and Environment. 2008;43:344-54.

[28] Livchak A, Nall D. Displacement ventilation–application for hot and humid climate. Proceedings of Clima2000.

[29] Riffat S, Zhao X, Doherty P. Review of research into and application of chilled ceilings and displacement ventilation systems in Europe. International Journal of Energy Research. 2004;28:257-86.

[30] Younis M, Ghali K, Ghaddar N. Performance evaluation of the displacement ventilation combined with evaporative cooled ceiling for a typical office in Beirut. Energy Conversion and Management. 2015;105:655-64.

[31] Wargocki P, Wyon DP, Sundell J, Clausen G, Fanger P. The effects of outdoor air supply rate in an office on perceived air quality, sick building syndrome (SBS) symptoms and productivity. Indoor air. 2000;10:222-36.

[32] Horikiri K, Yao Y, Yao J. Numerical study of unsteady airflow phenomena in a ventilated room. ICHMT DIGITAL LIBRARY ONLINE. 2012.

[33] Horikiri K, Yao Y, Yao J. Modelling conjugate flow and heat transfer in a ventilated room for indoor thermal comfort assessment. Building and Environment. 2014;77:135-47.

[34] Srebric J, Chen Q. Simplified numerical models for complex air supply diffusers. HVAC&R Research. 2002;8:277-94.

[35] Yuan X, Chen Q, Glicksman LR, Hu Y, Yang X. Measurements and computations of room airflow with displacement ventilation. Ashrae Transactions. 1999;105:340.

[36] Yakhot V, Orszag S, Thangam S, Gatski T, Speziale C. Development of turbulence models for shear flows by a double expansion technique. Physics of Fluids A: Fluid Dynamics (1989-1993). 1992;4:1510-20.

[37] Chandrasekhar S. Radiative heat transfer. Dover Publications, New York. 1960;11:11-2.

[38] Zhang Z, Chen Q. Comparison of the Eulerian and Lagrangian methods for predicting particle transport in enclosed spaces. Atmospheric Environment. 2007;41:5236-48.

[39] Fluent A. 14.5, Theory Guide; ANSYS. Inc, Canonsburg, PA. 2012.

[40] Nazaroff WW. Indoor particle dynamics. Indoor air. 2004;14:175-83.

[41] Li A, Ahmadi G. Dispersion and deposition of spherical particles from point sources in a turbulent channel flow. Aerosol Science and Technology. 1992;16:209-26.

[42] McLaughlin JB. Aerosol particle deposition in numerically simulated channel flow. Physics of Fluids A: Fluid Dynamics (1989-1993). 1989;1:1211-24.

[43] Nazaroff WW, Cass GR. Mathematical modeling of indoor aerosol dynamics. Environmental Science & Technology. 1989;23:157-66.

[44] Rizk M, Elghobashi S. The motion of a spherical particle suspended in a turbulent flow near a plane wall. Physics of Fluids (1958-1988). 1985;28:806-17.

[45] Wang M, Lin C-H, Chen Q. Advanced turbulence models for predicting particle transport in enclosed environments. Building and Environment. 2012;47:40-9.

[46] Romano F, Marocco L, Gustén J, Joppolo CM. Numerical and experimental analysis of airborne particles control in an operating theater. Building and Environment. 2015;89:369-79.

[47] Hinds WC. Aerosol technology: properties, behavior, and measurement of airborne particles. New York, Wiley-Interscience, 1982 442 p. 1982;1.

[48] Xu Y, Yang X, Yang C, Srebric J. Contaminant dispersion with personal displacement ventilation, Part I: Base case study. Building and Environment. 2009;44:2121-8.

[49] Chen F, Simon C, Lai AC. Modeling particle distribution and deposition in indoor environments with a new drift–flux model. Atmospheric Environment. 2006;40:357-67.

[50] Cao G, Awbi H, Yao R, Fan Y, Sirén K, Kosonen R et al. A review of the performance of different ventilation and airflow distribution systems in buildings. Building and Environment. 2014;73:171-86.

[51] Chen Q, Glicksman L. System performance evaluation and design guidelines for displacement ventilation:[prepared under ASHRAE research project 949...]: American Society of Heating, Refrigerating, and Air-Conditioning Engineers, Incorporated; 2003.

[52] ASHRAE A. Standard 55-2004, Thermal Environmental Conditions for Human Occupancy, Atlanta: American Society of Heating, Refrigerating, and Air-conditioning Engineers. Inc, USA. 2004.

[53] Fanger PO, Melikov AK, Hanzawa H, Ring J. Air turbulence and sensation of draught. Energy and buildings. 1988;12:21-39.

[54] Melikov AK, Langkilde G, Derbiszewski B. Airflow characteristics in the occupied zone of rooms with displacement ventilation. ASHR a E Transactions. 1990.

[55] Standard I. 7730. Ergonomics of the thermal environment—Analytical determination and interpretation of thermal comfort using calculation of the PMV and PPD indices and local thermal comfort criteria. International Organization for Standardization: Geneva, Switzerland2005.

[56] Chen H, Moshfegh B, Cehlin M. Computational investigation on the factors influencing thermal comfort for impinging jet ventilation. Building and Environment. 2013;66:29-41.

[57] Chen H, Moshfegh B, Cehlin M. Investigation on the flow and thermal behavior of impinging jet ventilation systems in an office with different heat loads. Building and Environment. 2013;59:127-44.

[58] Melikov A, Pitchurov G, Naydenov K, Langkilde G. Field study on occupant comfort and the office thermal environment in rooms with displacement ventilation. Indoor air. 2005;15:205-14.

[59] Fathollahzadeh MH, Heidarinejad G, Pasdarshahri H. Prediction of thermal comfort, IAQ, and energy consumption in a dense occupancy environment with the under floor air distribution system. Building and Environment. 2015;90:96-104.